St. Venants Torsion Constant of Hot Rolled Steel Profiles and Position of the Shear Centre

M. Kraus[1] & R. Kindmann[1]
[1] Institute for Steel and Composite Structures, University of Bochum, Germany

ABSTRACT: The knowledge of the cross section properties is required for the static analysis using beam theory. For arbitrary cross sections the exact torsional values can only be determined analytically if the section has a basic geometry. For that reason in practice different formulae are often used to approximate the values when rolled sections are applied. In contrast the use of numerical methods, as for instance the finite element method (FEM), allows the determination of the accurate torsional values. The approximations partially show comparatively big discrepancies to the accurate values. For that reason the accurate torsional properties of different hot rolled cross sections as well as new formulae based on the numerical solutions are presented in this essay. The new formulae allow a more precise approximation of the St. Venants torsion constant than the existing ones.

1 INTRODUCTION

Bar members are often subjected by torsional loadings. This especially applies for analyses according to 2nd order theory, since torsion not scheduled usually arises as shown in the example of Figure 1. For the static analysis using beam theory the knowledge of the torsional cross section properties is therefore essential.
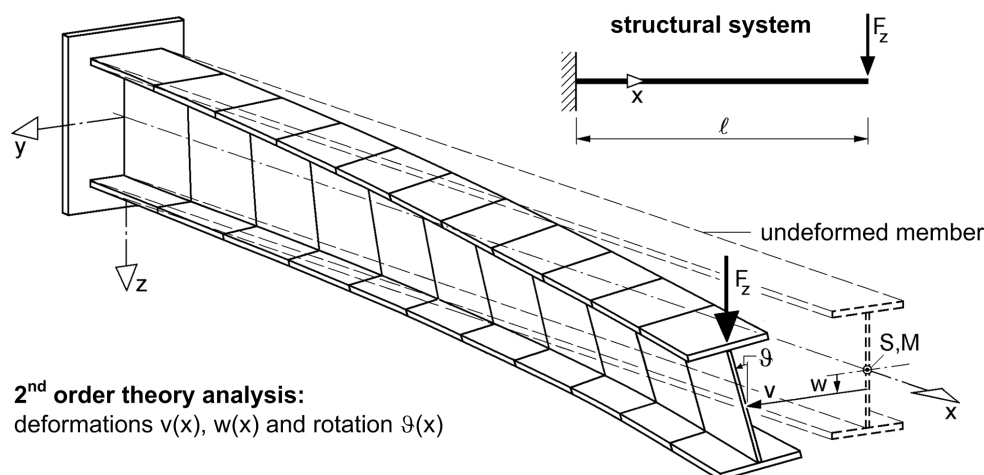

Figure 1. Deformation of a bar member according to 2nd order theory, Kindmann (2008)
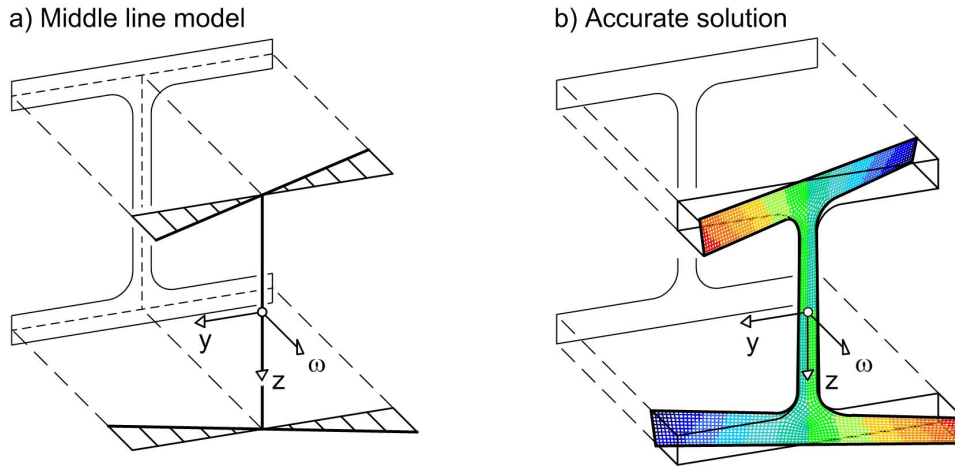
Figure 2. Warping ordinate of an HEM 200, Kraus (2005)

For rolled sections analytical solutions to determine these properties do not exist. For that reason the cross sections are assumed as thin walled in general and analyzed with corresponding theories and constitutive models. This leads to torsional properties which show discrepancies in comparison to accurate solutions, which can be determined using the finite element method (FEM). Figure 2 exemplifies the differences with the warping ordinate ω for a rolled I profile. The warping ordinate is a value, which connects the torque arising due to torsional loadings with the deformations u in longitudinal direction x of a bar:

$$u = -\omega(y,z) \cdot \vartheta'(x) \qquad (1)$$

Since the cross section does not keep a plane constitution when deforming, the distortions are referred to as warping. Using formula (1) ω can also be interpreted as unit warping for $\vartheta' = -1$. The deformation u resp. the warping ordinate depends on the position of the rotation axis, about which the cross section twists when subjected to torsion. In general this is the axis of the shear centre M to which the warping ordinate therefore refers to. Since the exact position is usually not known in advance, an arbitrary rotation axis D is chosen for which ordinates $\bar{\omega}$ can be determined either using the simplified models (middle line model/thin walled theory) or accurate approaches on basis of numerical models. The formulae

$$y_M - y_D = \frac{1}{I_y} \cdot \int_A z \cdot \bar{\omega} \cdot dA, \qquad z_M - z_D = -\frac{1}{I_z} \cdot \int_A y \cdot \bar{\omega} \cdot dA \qquad (2)$$

describe the position of the shear centre depending on $\bar{\omega}$. Now the warping ordinate can be determined by the following transformation relationship:

$$\omega = \bar{\omega} - \bar{\omega}_k - z \cdot (y_M - y_D) + y \cdot (z_M - z_D) \quad \text{with} \quad \bar{\omega}_k = \frac{1}{A} \cdot \int_A \bar{\omega} \cdot dA \qquad (3)$$

Figure 2 clarifies, that the accurate solution for the warping ordinate shows linearly changing values over the plate thickness. In contrast the solution using the middle line model only provides a single value which is assumed as constant regarding the plate thickness. This difference not only effects the position of the shear centre when regarding cross sections with less than two axes of symmetry, but also the St. Venants torsion constant as well as the warping constant. According to Kindmann & Kraus (2007) these values can be determined using the following formulae:

$$I_\omega = \int_A \omega^2 \cdot dA \qquad (4)$$

$$I_T = \int_A \left[\left(-\frac{\partial \omega}{\partial z} + (y - y_M) \right) \cdot (y - y_M) + \left(\frac{\partial \omega}{\partial y} + (z - z_M) \right) \cdot (z - z_M) \right] \cdot dA \qquad (5)$$

In the following chapters the determination of the torsional cross section properties, especially the St. Venants torsion constant will be focused on. Accurate results are compiled for different cross sections which were gained using the FEM. The knowledge of these values allows a development of formulae for approximation which provide better results than the existing ones so far.

455

2 FINITE ELEMENT METHOD FOR CROSS SECTIONS

The cross section properties presented in this essay are calculated with the program QSW-FE, see Kraus (2005). The theoretical background for the calculation of the properties as well as shear stresses due to shear forces, primary and secondary torsion using the finite element method (FEM) is also described by Kindmann & Kraus (2007) in detail. For that reason only the basic principles will be shown here.
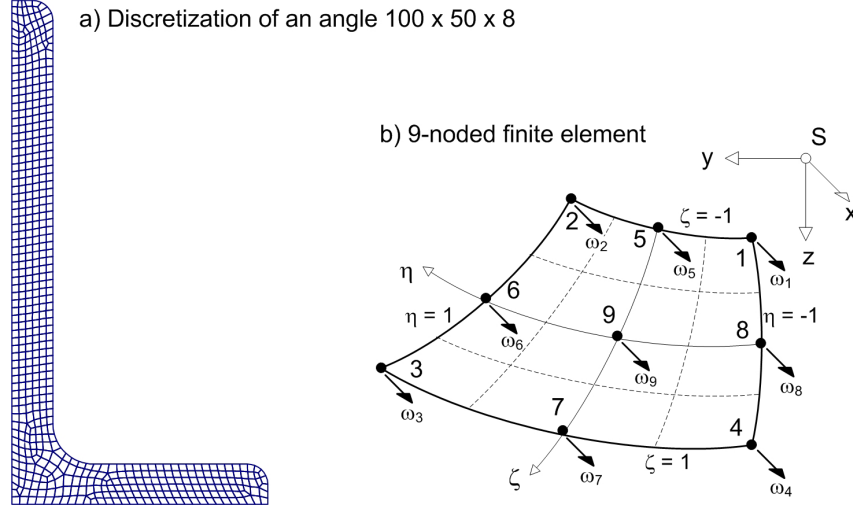

Figure 3. Discretization of a cross section using 9-noded finite elements

The cross section is divided into finite elements as shown in Figure 3 using curvilinear 9-noded elements. The element formulation is based on the isoparametric concept, where for the deformations as well as the element geometry an equal set of shape functions is used. In principle, elements with different numbers of nodes n could also be derived, the 9-noded element has exposed as very efficient in the sense of the numerical effort though. The degree of freedom in each node is the warping ordinate ω. The equilibrium in terms of virtual work for the cross section deformation due to primary torsion, to which the warping ordinate corresponds, can be stated for a finite element with the element area A_e as follows:

$$\delta W = \sum_{i=1}^{9} \delta\omega_i \cdot T_{xi}^* - G \cdot \int_{A_e} \left(\frac{\partial(\delta\omega)}{\partial z} \cdot \frac{\partial\omega}{\partial z} + \frac{\partial(\delta\omega)}{\partial y} \cdot \frac{\partial\omega}{\partial y} \right) \cdot dA_e$$
$$+ G \cdot \int_{A_e} \left(\frac{\partial(\delta\omega)}{\partial z} \cdot (y - y_M) - \frac{\partial(\delta\omega)}{\partial y} \cdot (z - z_M) \right) \cdot dA_e = 0 \tag{6}$$

The first component of this equation corresponds to an external virtual work, where the nodal shear flow T_x^*, which corresponds to the torque of $\vartheta' = -1$, accomplishes work at the warping ω. This shear flow is used to formulate the nodal equilibrium with regard to the whole element mesh yielding in the equation system for the cross section. The other components of formula (6) are gained from an inner virtual work, corresponding to $\vartheta' = -1$ as well. From these an element stiffness matrix and a kind of load vector can be formulated. The virtual work demands C^0-continuos shape functions which are summarized in the vector $\underline{f}$. The so called Lagrangian polynomials are applied with a quartic development corresponding to the 9-noded element. Equation (6) leads to the following element stiffness relationship with the element stiffness matrix $\underline{K}_e$ and the load vector $\underline{f}_{\vartheta'e}$:

$$\delta\underline{\omega}_e: \quad \underline{t}_{\tau e}^* = \underline{K}_e \cdot \underline{\omega}_e - \underline{f}_{\vartheta'e} \tag{7}$$

$$\underline{K}_e = G \cdot \int_{-1}^{1}\int_{-1}^{1} \left(\frac{\partial \underline{f}^T}{\partial z} \cdot \frac{\partial \underline{f}}{\partial z} + \frac{\partial \underline{f}^T}{\partial y} \cdot \frac{\partial \underline{f}}{\partial y} \right) \cdot \det(\underline{J}) \cdot d\eta \cdot d\zeta \tag{8}$$

$$\underline{f}_{\vartheta'e} = G \cdot \int_{-1}^{1}\int_{-1}^{1} \left\{ \frac{\partial \underline{f}^T}{\partial z} \cdot \left[(\underline{f} \cdot \underline{y}_e) - y_M \right] - \frac{\partial \underline{f}^T}{\partial y} \cdot \left[(\underline{f} \cdot \underline{z}_e) - z_M \right] \right\} \cdot \det(\underline{J}) \cdot d\eta \cdot d\zeta \tag{9}$$

The indication "$\delta\omega_e$:" in equation (8) is supposed to show, that the complete stiffness relationship depends on the virtual nodal values of the warping. The so called Jacobi determinant $\det(\underline{J})$ transforms the differential of the area $dA_e = dx \cdot dy$ in $d\eta \cdot d\zeta$. In addition the partial differentiations occurring in the formulae (8) and (9) have to be transformed as well, see Kraus (2007) for instance. The integrations can usually not be solved analytically. For that reason numerical integrations are performed using the Gauss quadrature.

After setting up the equation system using these element stiffness relationships the finite element calculation provides the warping ordinate referring to a reference point D at first, compare section 1. In order to determine the position of the shear centre, the St. Venants torsion constant and the warping constant, the integrations of the formulae (2) to (5) have to be solved. For that reason it is necessary to know the course of the function ω resp. $\bar{\omega}$ within the total cross section. However, the finite element analysis only provides the nodal solutions. For the description of the development within the finite elements the previously mentioned shape functions are applied again, as it is common use in numerical methods. With the knowledge of the warping ordinate the stresses due to primary torsional moments can also be determined.

Apparently the 9-noded element taking quartic functions as a basis for the deformation will provide a certain inaccuracy, since the real distortional behavior will differ in general. In addition further factors will influence the exactness of the FEM-solution using two-dimensional curvilinear elements. Detailed information to this issue is given by Kindmann & Kraus (2007). With a refinement of the element mesh the inaccuracies can be minimized leading to FEM-results with high accuracy.

3 DOUBLESYMMETRIC I-SECTIONS

3.1 *Accurate cross section properties*

In Table 1 the accurate results of the torsional cross section properties are compiled for rolled I sections. The values are gained as described in the previous chapter. Kindmann et al. (2008) and Wagner et al. (1999) have published further results for a great variety of cross sections.

Table 1. Accurate torsional cross section properties for rolled I-sections

|	IPE				HEA			HEB			HEM		
profile	I_T cm^4	I_ω cm^6	max ω cm^2	profile	I_T cm^4	I_ω cm^6	max ω cm^2	I_T cm^4	I_ω cm^6	max ω cm^2	I_T cm^4	I_ω cm^6	max ω cm^2
80	0,6727	115,1	8,516	100	5,199	2 475	21,65	9,309	3 233	22,12	67,28	9 430	25,91
100	1,153	342,1	12,82	120	5,957	6 285	31,45	13,94	9 125	32,31	90,53	23 887	36,88
120	1,689	872,0	18,04	140	8,032	14 729	43,21	20,20	21 965	44,39	118,6	52 826	49,74
140	2,401	1 951	24,14	160	11,84	30 615	56,65	31,24	46 667	58,19	160,8	104 700	64,28
160	3,530	3 889	31,06	180	14,66	59 014	72,13	42,24	91 728	74,07	201,4	194 300	80,94
180	4,723	7 322	38,90	200	20,43	105 580	89,25	59,59	167 060	91,65	258,1	336 870	99,28
200	6,846	12 746	47,50	220	28,09	189 610	108,7	77,02	289 510	111,3	313,6	559 550	119,7
220	8,982	22 310	57,59	240	41,03	321 640	129,8	103,6	476 280	132,7	627,2	1 123 500	146,0
240	12,74	36 680	68,51	260	52,00	504 990	153,1	125,7	736 280	156,2	722,3	1 684 000	170,7
270	15,71	69 469	87,12	280	61,39	770 140	178,6	145,3	1 107 200	182,0	809,4	2 463 000	197,5
300	19,75	124 260	107,9	300	84,24	1 174 700	205,4	187,4	1 651 000	209,0	1 415	4 280 100	230,9
330	27,59	196 090	126,6	320	108,8	1 482 600	219,2	229,2	2 026 200	222,9	1 510	4 890 000	244,0
360	37,08	309 370	146,8	340	128,7	1 790 200	233,5	262,0	2 405 600	237,1	1 516	5 463 300	257,9
400	50,41	482 890	172,9	360	151,0	2 137 700	247,7	297,9	2 829 300	251,3	1 517	6 009 300	270,9
450	66,05	780 970	205,7	400	191,4	2 893 600	276,5	361,1	3 751 100	280,1	1 524	7 268 800	298,5
500	88,62	1 235 400	240,9	450	249,1	4 087 200	312,5	448,9	5 177 700	316,1	1 538	9 092 300	333,8
550	121,7	1 861 500	278,3	500	317,7	5 569 200	348,5	549,9	6 920 700	352,1	1 548	11 012 000	367,9
600	164,6	2 814 700	318,0	550	360,6	7 103 100	385,2	612,3	8 743 900	388,8	1 563	13 323 000	404,6
				600	407,5	8 879 600	421,9	679,6	10 838 000	425,5	1 574	15 700 000	439,8
				650	458,6	10 915 000	458,6	752,0	13 219 000	462,2	1 588	18 427 000	476,4
				700	522,8	13 223 000	495,3	841,7	15 900 000	498,9	1 599	21 161 000	511,4
				800	609,6	18 113 000	569,2	962,1	21 617 000	572,7	1 663	27 472 000	583,5
				900	751,0	24 748 000	642,6	1 154	29 196 000	646,2	1 689	34 419 000	654,1
				1000	837,3	31 834 000	716,8	1 272	37 340 000	720,4	1 719	42 665 000	728,1
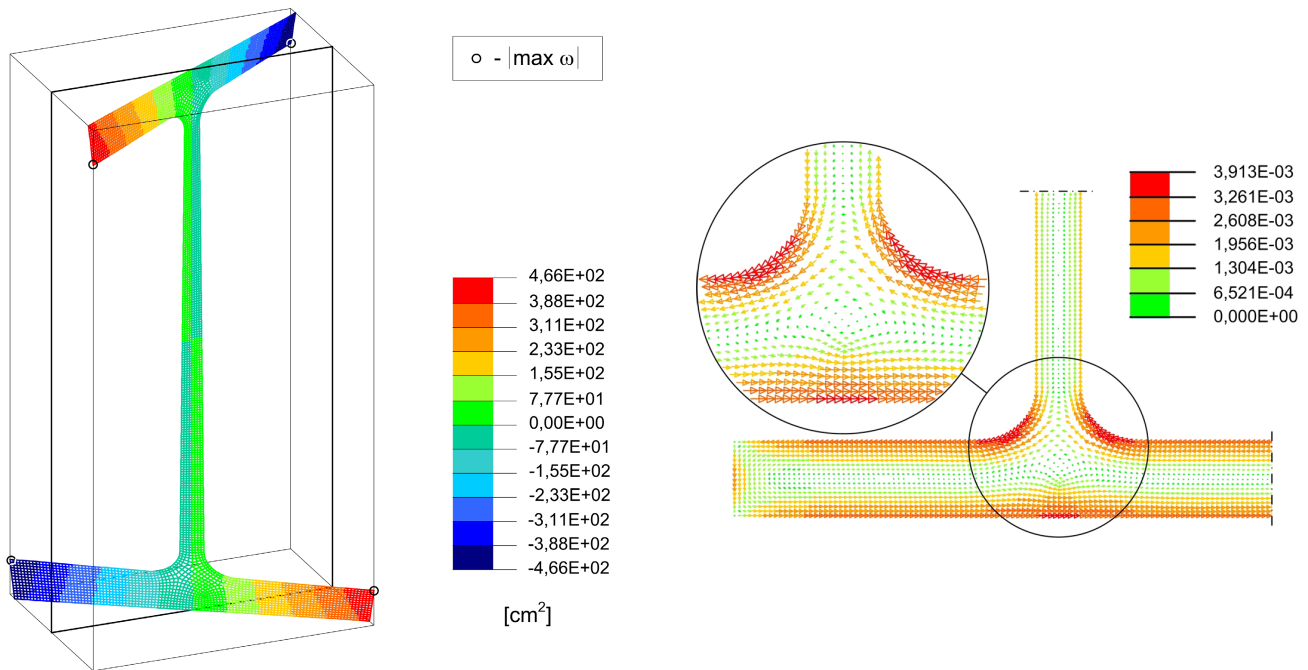
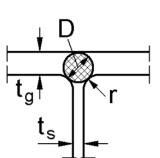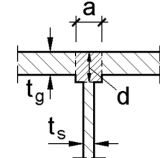Figure 4. Warping ordinate (HEM 600) and shear stresses as a result of St. Venants torsion (HEM 300)
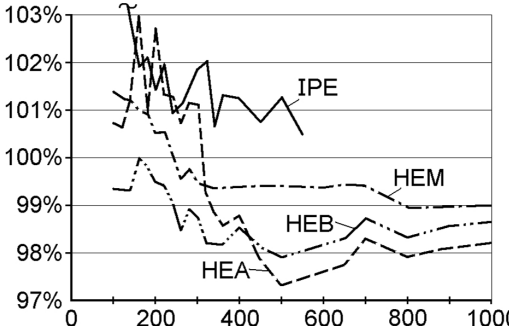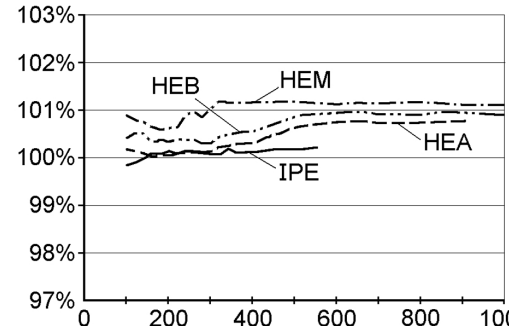
Concerning Table 1 it should be mentioned, that max ω specifies the maximum warping ordinate. However, here the maximum value of the plate middle line is compiled, even though the values at the plate edges are bigger. Figure 4 (left) is supposed to clarify this issue. It shows the numerical result for the warping ordinate for an HEM 600. The maximum value of 466 cm^2 is located at the plate edge. The value of 439.8 cm^2 specified in Table 1 is the warping at mid-plate.

It is an interesting aspect that if a middle line model is applied, not regarding the rolled areas going along with a smaller cross section area, larger values for I_ω are determined for the cross sections of Table 1. Kraus (2005) analyzes this phenomenon. It is a result of the warping behavior of the cross section. The rolled areas lead to a smaller cross section warping. When integrating to I_ω according to formula (5), this effect has a larger influence than the gain of the cross section area.

3.2 New formula for the St. Venants torsion constant

Figure 4 shows finite element solution for a hot rolled I-section. The figure on the right displays the shear stress distribution for a HEM 300 due to a primary torsion moment $M_{xp} = 1$ kNcm. In the area

Table 2 Past and new formula for the I_T of rolled I-sections

Past formula	New formula
$I_T = \dfrac{2}{3} \cdot b \cdot t_g^3 \cdot \left(1 - 0.63 \cdot \dfrac{t_g}{b}\right) + \dfrac{1}{3}\left(h - 2 \cdot t_g\right) \cdot t_s^3 + 2 \cdot \alpha \cdot D^4$	$I_T = \dfrac{2}{3} \cdot t_g^3 \cdot (b - a) + \dfrac{1}{3}\left(h - 2 \cdot d\right) \cdot t_s^3 + \alpha \cdot d^3 \cdot a$
$D = \dfrac{\left(t_g + r\right)^2 + t_s \cdot \left(r + t_s / 4\right)}{2 \cdot r + t_g}$ $\alpha = \left(0.1 \cdot \dfrac{r}{t_g} + 0.145\right) \cdot \dfrac{t_s}{t_g}$	$d = D; \quad a = t_s + \dfrac{r^2}{d - t_g} \cdot \dfrac{4 - \pi}{2}$ $\alpha = 0.46 - 0.5\left(d/a - 1.15\right)^2$

458

of the transition from web to flange (rolled area), a concentration of stresses can be recognized. It is obvious that this is going along with an increased torsion stiffness resp. I_T, which cannot be covered by modeling the cross section using rectangular partial plates, which is a common approach for the calculation of I_T. For this purpose Trayer & March (1930) develop a formula on basis of the membrane analogy. In this model the flanges and the web are covered by rectangular partial plates. In addition, to cover the stress concentration within the rolled area, Trayer & March overlap a circle with the diameter D. The portion of the torsional constant from this additional part is modified by a factor α. It should be mentioned, that this proceeding is not in conformance to the usual approach of dividing into independent partial areas. However, the priory interest is the accuracy of the calculation formula. For that purpose the numerical solutions are comparatively referred to. As shown in Table 1, the accuracy of the formula is between 97.4 and 104.3 % for the common European rolled series IPE, HEA, HEB and HEM. However, further calculations for other profiles show much larger discrepancies. The largest one noticed is for an HP 320 x 88, where the formula delivers a value of $I_T = 99.04$ cm^4, while the FEM calculation provides $I_T = 76.84$ cm^4, being a not negligible overestimation (129 %). For that reason Kindmann (2006) works out a new formula, with which the St. Venants torsion constant can be determined with higher accuracy. Table 1 displays the new formula in comparison to the one of Trayer & March. In the new model the partial areas of the cross section, which are used to determine I_T, do not overlap.

4 ANGLES

4.1 *Accurate cross section properties and position of the shear centre*

Usually angles are treated free of warping, being a result of the assumption of a thin walled cross section (middle line model). Calculations on bases of the FEM show, that due to the actual plate thickness the angles show warping deformations, although being relatively small. However, the deformations have an influence on the position of the shear centre M. While regarding the middle line model, M is positioned at the intersection of the middle lines of the angle legs. Table 4, with reference to Figure 6, gives an overview on where the accurate position of the shear center in comparison to the middle line model is. In addition, Table 4 contains the results for the torsional constant.
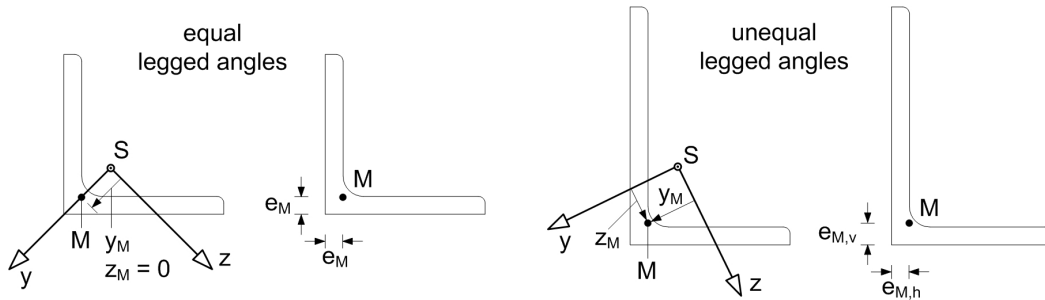

Figure 6. Position of the shear center of equal and unequal legged angels

4.2 *New formula for the St. Venants torsion constant*

Angles also show stress concentrations due to primary torsional moments in the rolled area as shown for I-sections, compare Figure 7. For the determination of the St. Venants torsion constant two approaches have been followed in the past. In the first one only the partial rectangular plates are regarded for each angle leg leading to the following formula:

$$I_T = 1/3 \cdot (a + b - t) \cdot t^3 \tag{10}$$

The second approach corresponds to the formula of the I-sections, where an additional circle is inserted to cover the torsional rigidity of the rolled areas, see Petersen (1990) for example:

$$I_T = a \cdot \frac{t^3}{3} \cdot (1 - 0.315 \cdot t/a) + (b - t) \cdot \frac{t^3}{3} \cdot \left(1 - 0.315 \cdot \frac{t}{b - t}\right) + \alpha \cdot D^4 \tag{11}$$

with: $D = 2 \cdot (2 \cdot t + 3 \cdot r) - \sqrt{8 \cdot (t + 2 \cdot r)^2}$, $\alpha = 0.07 \cdot r/t + 0.076$

Table 3. Accurate torsional cross section properties for rolled angles according to DIN EN 10056-1.

Dimensions a×a×t in mm (short symbol)	y_M FEM cm	ML cm	AW %	e_M FEM cm	I_T FEM cm^4
20×20×3	0,578	0,634	9,7	0,190	0,0370
25×25×3	0,766	0,810	5,8	0,181	0,0460
4	0,734	0,795	8,2	0,243	0,1038
30×30×3	0,913	0,969	6,1	0,189	0,0596
4	0,888	0,960	8,0	0,250	0,1332
35×35×4	1,075	1,136	5,6	0,243	0,1545
40×40×4	1,235	1,301	5,3	0,246	0,1829
5	1,210	1,290	6,6	0,306	0,3430
45×45×4,5	1,383	1,460	5,5	0,279	0,2959
50×50×4	1,576	1,639	4,0	0,245	0,2342
5	1,556	1,631	4,8	0,303	0,4393
6	1,531	1,620	5,8	0,363	0,7359
60×60×5	1,898	1,971	3,9	0,302	0,5379
6	1,877	1,962	4,5	0,360	0,9014
8	1,823	1,936	6,2	0,480	2,040
65×65×7	2,014	2,117	5,1	0,423	1,544
70×70×6	2,219	2,303	3,8	0,359	1,070
7	2,197	2,293	4,3	0,417	1,658
75×75×6	2,401	2,479	3,2	0,355	1,142
8	2,356	2,457	4,3	0,471	2,595
80×80×8	2,518	2,623	4,2	0,475	2,814
10	2,464	2,597	5,4	0,594	5,313
90×90×7	2,880	2,973	3,2	0,416	2,195
8	2,861	2,965	3,6	0,474	3,209
9	2,838	2,954	4,1	0,532	4,489
10	2,813	2,941	4,6	0,591	6,063
100×100×8	3,201	3,305	3,2	0,473	3,609
10	3,158	3,284	4,0	0,589	6,820
12	3,105	3,257	4,9	0,708	11,48
120×120×10	3,865	3,979	3,0	0,581	8,253
12	3,819	3,955	3,6	0,696	13,92
130×130×12	4,163	4,298	3,3	0,696	15,23
150×150×10	4,881	4,998	2,4	0,582	10,61
12	4,846	4,982	2,8	0,696	17,88
15	4,778	4,946	3,5	0,869	33,92
160×160×15	5,123	5,290	3,3	0,868	36,47
180×180×16	5,806	5,973	2,9	0,918	49,71
18	5,757	5,946	3,3	1,034	69,77
200×200×16	6,529	6,679	2,3	0,906	55,17
18	6,483	6,653	2,6	1,020	77,55
20	6,433	6,623	3,0	1,135	105,1
24	6,321	6,559	3,8	1,368	177,8
250×250×28	8,029	8,260	2,9	1,564	350,1
35	7,813	8,132	4,1	1,976	666,3

Dimensions a×b×t in mm (short symbol)	y_M FEM cm	ML cm	AW %	z_M FEM cm	ML cm	AW %	$e_{M,h}$ FEM cm	$e_{M,v}$ FEM cm	I_T FEM cm^4
30×20×3	0,610	0,653	7,1	0,575	0,634	10,2	0,167	0,221	0,0473
4	0,580	0,637	9,8	0,546	0,634	16,1	0,218	0,303	0,1062
40×20×4	0,544	0,581	6,9	1,016	1,159	14,0	0,202	0,347	0,1275
40×25×4	0,767	0,809	5,4	0,857	0,936	9,3	0,211	0,289	0,1382
45×30×4	0,959	1,002	4,4	0,896	0,958	6,9	0,214	0,274	0,1622
50×30×5	0,903	0,954	5,7	1,119	1,230	9,9	0,261	0,372	0,3321
60×30×5	0,858	0,897	4,6	1,599	1,747	9,2	0,251	0,403	0,3737
60×40×5	1,287	1,340	4,2	1,202	1,278	6,3	0,269	0,340	0,4263
6	1,261	1,325	5,1	1,180	1,278	8,3	0,320	0,415	0,7174
65×50×5	1,690	1,741	3,0	0,967	1,008	4,3	0,273	0,311	0,4888
70×50×6	1,640	1,705	4,0	1,237	1,310	5,9	0,326	0,394	0,8799
75×50×6	1,624	1,684	3,7	1,514	1,599	5,6	0,321	0,402	0,9159
8	1,571	1,651	5,1	1,468	1,599	8,9	0,422	0,552	2,087
80×40×6	1,154	1,204	4,4	2,155	2,326	7,9	0,306	0,478	0,8799
8	1,102	1,169	6,0	2,055	2,325	13,1	0,398	0,678	2,002
80×60×7	1,988	2,064	3,9	1,261	1,332	5,6	0,383	0,449	1,625
100×50×6	1,487	1,534	3,2	2,767	2,914	5,3	0,308	0,453	1,117
8	1,443	1,503	4,2	2,688	2,914	8,4	0,402	0,634	2,552
100×65×7	2,100	2,177	3,6	2,107	2,214	5,1	0,379	0,478	1,981
8	2,080	2,165	4,1	2,087	2,215	6,1	0,430	0,551	2,899
10	2,029	2,134	5,2	2,039	2,216	8,7	0,530	0,704	5,480
100×75×8	2,502	2,590	3,5	1,586	1,665	5,0	0,439	0,511	3,070
10	2,452	2,561	4,5	1,558	1,666	6,9	0,544	0,647	5,813
12	2,393	2,527	5,6	1,523	1,666	9,4	0,650	0,789	9,786
120×80×8	2,637	2,717	3,0	2,454	2,559	4,3	0,431	0,528	3,550
10	2,593	2,691	3,8	2,417	2,560	5,9	0,532	0,670	6,730
12	2,540	2,657	4,6	2,372	2,560	7,9	0,633	0,819	11,35
125×75×8	2,393	2,467	3,1	2,948	3,083	4,6	0,424	0,553	3,550
10	2,350	2,440	3,8	2,899	3,085	6,4	0,522	0,705	6,730
12	2,297	2,406	4,7	2,838	3,084	8,6	0,620	0,868	11,35
135×65×8	1,894	1,957	3,3	3,819	4,033	5,6	0,410	0,623	3,550
10	1,852	1,929	4,1	3,736	4,035	8,0	0,503	0,808	6,730
150×75×9	2,230	2,301	3,2	4,151	4,371	5,3	0,462	0,680	5,657
10	2,210	2,287	3,5	4,116	4,372	6,2	0,510	0,767	7,654
12	2,164	2,255	4,2	4,032	4,371	8,4	0,603	0,951	12,92
15	2,083	2,197	5,5	3,876	4,366	12,6	0,741	1,253	24,48
150×90×10	2,887	2,970	2,9	3,547	3,708	4,5	0,523	0,680	8,154
12	2,841	2,939	3,5	3,497	3,708	6,0	0,621	0,832	13,78
15	2,759	2,884	4,5	3,403	3,706	8,9	0,767	1,077	26,17
150×100×10	3,332	3,417	2,6	3,088	3,207	3,9	0,530	0,643	8,487
12	3,286	3,388	3,1	3,052	3,208	5,1	0,631	0,783	14,36
200×100×10	3,025	3,101	2,5	5,615	5,833	3,9	0,517	0,730	10,48
12	2,991	3,078	2,9	5,556	5,837	5,1	0,613	0,894	17,70
15	2,925	3,032	3,6	5,441	5,837	7,3	0,753	1,160	33,65
200×150×12	5,189	5,287	1,9	3,255	3,342	2,7	0,644	0,724	20,58
15	5,124	5,247	2,4	3,224	3,343	3,7	0,799	0,914	39,27

FEM: Solution of the FEM
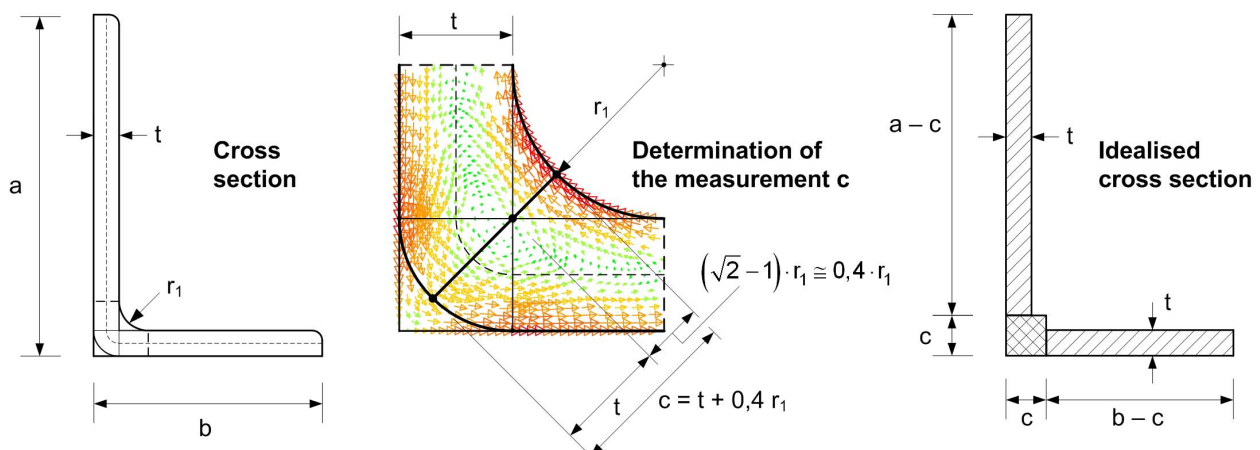ML: Solution of the middle line model
AW: Deviation (ML / FEM)

$$(\sqrt{2}-1)\cdot r_1 \cong 0,4\cdot r_1$$

$$c = t + 0,4\, r_1$$

Figure 7. Model for the determination of the new formula for I_T

equal legged angles

Eq. (10)
Eq. (11)
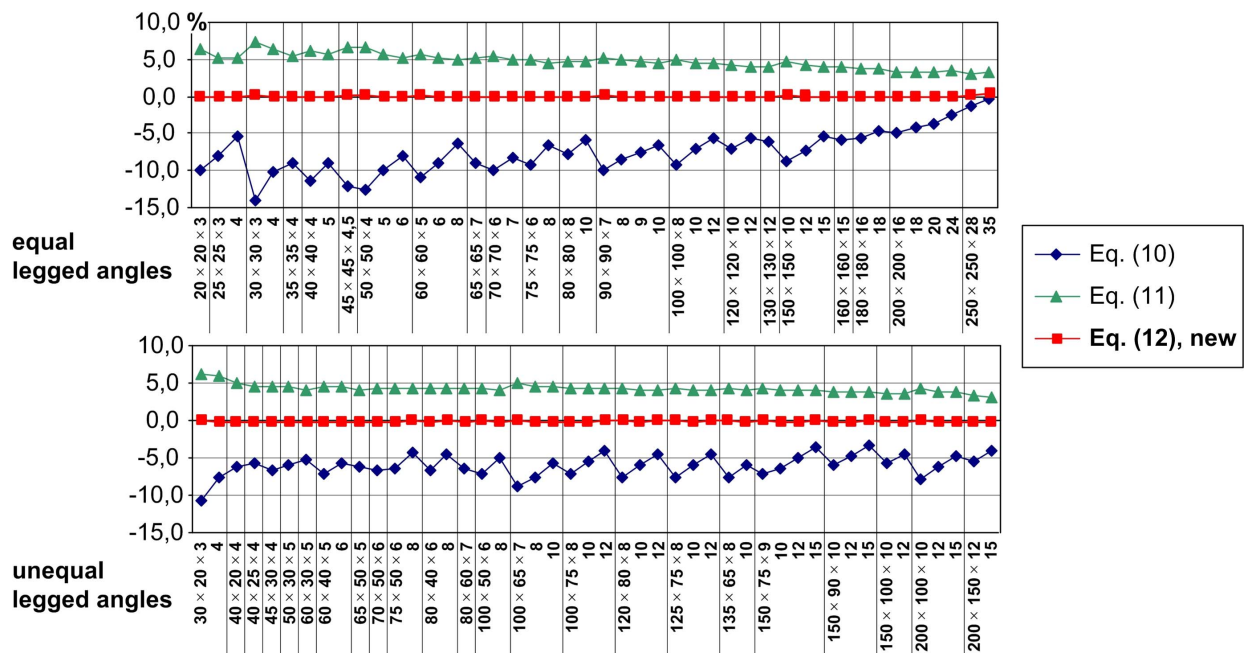**Eq. (12), new**

unequal legged angles

Figure 8. Discrepancies of the approximations for I_T

The deviation of the results gained by equation (10) and (11), in comparison to the accurate solution of the FEM, is displayed in Figure 8. Using formula (10) the largest discrepancy of about 14 % can be noticed, where the I_T is always calculated to small. On the other hand, the I_T using formula (11) is always approximated to large. For that reason Kindmann & Kraus (2008) develop a new formula, for which the basic idea of the I-sections is being picked up and the cross section is divided into three partial components as shown in Figure 7. The derivation leads to the following formula:

$$I_T = (a + b - 2 \cdot c) \cdot t^3 / 3 + 0.237 \cdot c^4 \qquad \text{with: } c = t + 0.4 \cdot r_1 \tag{12}$$

The results of this equation show a very good compliance to the FEM solution between 99.9 and 100.1 % for unequal- resp. 99.9 and 100.4 % for equal legged angles as shown in Figure 8.

5 CONCLUSIONS

With the finite element method accurate results for the torsional properties can be obtained contributing to the quality of the static analysis of bar members. For many profiles the accurate results are tabled in this essay in order to directly implement them to these analyses. In addition formulae were derived to provide aids for a quick determination of the torsional constant for similar profiles.

LITERATURE

Kindmann, R. 2006. Neue Berechnungsformel für das IT von Walzprofilen und Berechnung der Schubspannungen. *Stahlbau* 75 (2006): 371-374.
Kindmann, R., Kraus, M. 2007. *Finite-Elemente-Methoden im Stahlbau*. Berlin: Verlag Ernst & Sohn.
Kindmann, R. 2008. *Stahlbau, Teil 2: Stabilität und Theorie II. Ordnung*. Berlin: Verlag Ernst & Sohn.
Kindmann, R., Kraus, M. 2008. Torsionsträgheitsmoment und Schubmittelpunkt von Winkelprofilen. *Bautechnik* 85 (2008): 371-374.
Kindmann, R., Kraus, M., Niebuhr, H. J. (2nd ed.) 2008. *STAHLBAU KOMPAKT, Bemessungshilfen, Profiltabellen*. Düsseldorf: Verlag Stahleisen.
Kraus, M. 2005. *Computerorientierte Berechnungsmethoden für beliebige Stabquerschnitte des Stahlbaus*. Aachen: Shaker Verlag.
Kraus, M. 2007. On the Computation of Hot Rolled Cross Section Properties and Stresses using the Finite Element Method. *Proceedings of the 6th Int. Conf. on Steel & Aluminium Structures (ICSAS 2007)*: 409-416
Petersen, C. 1990. *Stahlbau*. Wiesbaden: Vieweg Verlag.
Trayer, G. W., March, H. W. 1930. Torsion of members having sections common in aircraft construction. *NACA-Report* 334.
Wagner, W., Sauer, R. Gruttmann, F. 1999. Tafeln der Torsionskenngrößen von Walzprofilen unter Verwendung von FE-Diskretisierungen. *Stahlbau* 68 (1999): 102-111.